Published in final edited form as:

Matrix Biol. 2024 January ; 125: 88–99. doi:10.1016/j.matbio.2023.12.005.

A role for decorin in improving motor deficits after traumatic brain injury

Kaori Oshima[1,*], **Noah Siddiqui**[2,*], **James E. Orfila**[3], **Danelle Carter**[4], **Justin Laing**[2], **Xiaorui Han**[5,6], **Igor Zakharevich**[7], **Renato V. Iozzo**[8], **Arsen Ghasabayan**[9], **Hunter Moore**[9], **Fuming Zhang**[5], **Robert J. Linhardt**[5], **Ernest E. Moore**[9], **Nidia Quillinan**[10], **Eric P. Schmidt**[1], **Paco S. Herson**[3], **Joseph A. Hippensteel**[2]

[1]Division of Pulmonary and Critical Care Medicine, Massachusetts General Hospital, Harvard Medical School, Boston, Massachusetts, USA.

[2]Division of Pulmonary Sciences and Critical Care Medicine, University of Colorado Anschutz Medical Campus, Aurora, Colorado, USA.

[3]Department of Neurosurgery, The Ohio State University College of Medicine, Columbus, Ohio, USA.

[4]Department of Neurology, University of Colorado Anschutz Medical Campus, Aurora, Colorado, USA.

[5]Departments of Chemistry and Chemical Biology, Chemical and Biological Engineering, and Biomedical Engineering, Rensselaer Polytechnic Institute, Troy, New York, USA.

[6]Curtin Medical School, Curtin Health Innovation Research Institute, Curtin University, Perth, Western Australia, Australia.

[7]Department of Biochemistry, University of Colorado Anschutz Medical Campus, Aurora, Colorado, USA.

[8]Department of Pathology and Genomic Medicine and the Translational Cellular Oncology Program, Sidney Kimmel Cancer Center, Sidney Kimmel Medical College at Thomas Jefferson University, Philadelphia, Pennsylvania, USA.

[9]Department of Surgery, Ernest E. Moore Shock Trauma Center at Denver Health, University of Colorado, Denver, Colorado, USA.

Corresponding Author: Joseph A. Hippensteel, joseph.hippensteel@cuanschutz.edu, **Permanent Address:** 12700 East 19th Ave, Research Complex 2, Mail Stop C232, Aurora, Colorado, USA 80045.

*Kaori Oshima and Noah Siddiqui contributed equally to this work.

Author Contribution

KO, NS, JEO, RVI, RJL, NQ, EPS, PSH, JAH conceived and planned the experiments. Animal experiments were performed by JAH, JEO, NS, JL, and DC. Mass spectrometry was performed by KO, XH, IZ and FZ. Human subjects were enrolled by AG, HM, and EEM. JAH, KO, NS, EPS, and PSH analyzed all data. KO, NS, and JAH wrote the manuscript with input from all authors. All authors reviewed and approved the final manuscript.

Declarations of Competing Interest

None

[10]Department of Anesthesiology, University of Colorado Anschutz Medical Campus, Aurora, Colorado, USA.

Abstract

Traumatic brain injury (TBI) is the leading cause of death and disability due to injury worldwide. Extracellular matrix (ECM) remodeling is known to significantly contribute to TBI pathophysiology. Glycosaminoglycans, which are long-chain, variably sulfated polysaccharides abundant within the ECM, have previously been shown to be substantially altered after TBI. In this study, we sought to delineate the dynamics of glycosaminoglycan alterations after TBI and discover the precise biologic processes responsible for observed glycosaminoglycan changes after injury. We performed state-of-the art mass spectrometry on brain tissues isolated from mice after TBI or craniotomy-alone. We observed dynamic changes in glycosaminoglycans at Day 1 and 7 post-TBI, with heparan sulfate, chondroitin sulfate, and hyaluronan remaining significantly increased after a week vis-à-vis craniotomy-alone tissues. We did not observe appreciable changes in circulating glycosaminoglycans in mice after experimental TBI compared to craniotomy-alone nor in patients with TBI and severe polytrauma compared to control patients with mild injuries, suggesting increases in injury site glycosaminoglycans are driven by local synthesis. We subsequently performed an unbiased whole genome transcriptomics analysis on mouse brain tissues 7 days post-TBI and discovered a significant induction of hyaluronan synthase 2, glypican-3, and decorin. The functional role of decorin after injury was further examined through multimodal behavioral testing comparing wild-type and *Dcn*$^{-/-}$ mice. We discovered that genetic ablation of *Dcn* led to an overall negative effect of TBI on function, exacerbating motor impairments after TBI. Collectively, our results provide a spatiotemporal characterization of post-TBI glycosaminoglycan alterations in the brain ECM and support an important adaptive role for decorin upregulation after TBI.

Keywords

Traumatic Brain Injury; Polytrauma; Glycosaminoglycans; Proteoglycans; Extracellular Matrix; Decorin; Glypican 3; Hyaluronan Synthase

Introduction

Traumatic brain injury (TBI) affects approximately 25 million people worldwide annually[1] and is the leading cause of death and disability due to injury[2]. While there have been significant efforts to ameliorate the impact of TBI via prevention programs, its societal importance continues to grow; between 2006 and 2014, TBI-related emergency department visits increased by greater than 50% in the United States[2]. Despite this burden, no pharmacologic therapies exist for the treatment of post-TBI brain dysfunction[3].

Extracellular matrix (ECM) remodeling is a hallmark of the biologic response to TBI [4, 5]. Glycosaminoglycans (GAGs) are a unique molecular family of variably sulfated polysaccharides that are a prevalent component of the ECM and highly bioactive. There are several classes of GAGs including heparan sulfate, chondroitin sulfate, and hyaluronan, which are defined by their specific constituent repeating disaccharide subunits. Heparan

sulfate and chondroitin sulfate disaccharide residues are variably sulfated and are typically covalently attached to a protein core—molecules referred to collectively as proteoglycans[6]. In contrast, the GAG hyaluronan is neither sulfated nor covalently bound to a protein. Substantial alterations in GAG and proteoglycan composition of the ECM have been reported to occur after TBI[4]. Our group has performed detailed analyses of GAG structure and function in healthy and injured biologic tissues (including blood and brain) through application of state-of-the-art mass spectrometry techniques[7–11].

GAG levels have previously been quantified in a stab wound model of brain injury using mass spectrometry. This prior work demonstrated increases in both chondroitin sulfate[12] and heparan sulfate[13] although the direct relevance of these findings to TBI has not been validated. Furthermore, several groups have measured chondroitin sulfate in translationally relevant pre-clinical TBI models using indirect quantification methods (e.g., non-specific immunoassays)[14, 15] and provided insights into relative disaccharide sulfation percentages using mass spectrometry[16], yet absolute quantification of chondroitin sulfate has not been performed in these models. This is significant as a growing body of evidence suggests targeting chondroitin sulfate is therapeutically promising after TBI[17]. Additionally, while there is indirect evidence that hyaluronan synthesis increases at the site of injury after TBI[18], to our knowledge, quantitative methods have not been applied to directly measure levels at the site of injury. Similarly, quantification of heparan sulfate levels have not been reported in translationally relevant models of TBI.

While a local inflammatory response to injury is a major contributor to dynamics of ECM and GAG remodeling after brain injury, TBI can also elicit an exuberant systemic inflammatory response, particularly when coincident with severe bodily injury in the form of polytrauma[19–24]. Recently, we discovered that systemic inflammation like sepsis leads to release of GAGs into the bloodstream from the endothelial glycocalyx of systemic vasculature[9, 25, 26]. These GAGs selectively penetrate the brain barrier, where they inhibit a key neurotrophic pathway, and negatively affect cognition[7, 8]. Interestingly, there is compelling evidence that extracranial injury, such as polytrauma, can directly aggravate functional outcomes in TBI survivors[24, 27]. TBI accompanied by polytrauma has also been associated with significant endothelial injury[28, 29]. Accordingly, observed associations between polytrauma and worsened TBI outcomes could be driven by pathogenic, brain-penetrating circulating factors released from injured endothelial cells, including glycocalyx-derived GAGs.

Based upon the known roles of both dynamic GAG remodeling of the ECM and systemic inflammation in the pathophysiology of TBI with and without concomitant traumatic injury, we hypothesized that, similar to sepsis, endothelial glycocalyx-derived GAGs are released into the circulation early in TBI, deposit within the brain, and contribute to compositional ECM changes. We tested this hypothesis by pairing quantification of GAGs via high performance liquid chromatography tandem mass spectrometry multiple reaction monitoring (HPLC-MS/MS) with bulk transcriptomic analyses of brain tissues and plasma collected from a murine model of TBI. Our pre-clinical findings were corroborated with quantification of GAGs in human plasma samples, comparing levels in patients affected by polytrauma and TBI—those at highest risk for systemic inflammation and resultant endothelial injury—to

those with mild traumatic injury without TBI. Lastly, we tested the functional significance of glycobiological changes at the site of brain injury utilizing transgenic mice in a multimodal behavioral model.

Results

Experimental traumatic brain injury significantly alters GAG content at the damaged site

We subjected mice to either craniotomy followed by controlled-cortical impact (TBI) or craniotomy alone (control). One or seven days later, we explanted the whole brains under terminal anesthesia (Fig. 1). One day after surgery, brain injury was grossly apparent after TBI and, to a lesser extent, after craniotomy alone. The TBI group had large sites of hemorrhage and minor tissue defects at the site of cortical impact, whereas the craniotomy group had mild erythema without an accompanying tissue defect. Observed injury in the craniotomy "control" group early after surgery demonstrates the susceptibility of the ipsilateral brain to "sham" insults, consistent with previous reports[30, 31]. After 7 days, TBI-treated brains remained erythematous with approximately 1 mm of tissue destruction at the site of cortical impact, whereas the craniotomy group appeared grossly normal.

One or seven days after surgery, several brain regions were isolated from mice. Two layers (superficial and deep) were isolated from the brain ipsilateral to injury and compared to intact tissues contralateral to the site of injury. "Superficial ipsilateral" tissue was harvested from a location at the site of injury that corresponded to the depth of cortex prior to injury; contralateral cortical tissue was also isolated from these animals and designated "superficial contralateral". "Deep ipsilateral" tissues were harvested from an area that corresponded to the location of the hippocampus prior to injury (although its typical structure was no longer intact in TBI tissue); contralateral hippocampal tissue was also harvested from these animals and designated "deep contralateral". Cortical (superficial) and hippocampal (deep) tissue were collected from animals after craniotomy from both ipsilateral (directly adjacent to craniotomy site) and contralateral hemispheres. We measured GAG content (heparan sulfate, chondroitin sulfate, and hyaluronan) and disaccharide sulfation patterns via HPLC-MS/MS in all collected samples. These analyses revealed temporally dynamic changes in GAG subtypes after TBI, but no significant changes after craniotomy alone. There were no significant changes in heparan sulfate levels at day 1 in superficial (Fig 2a) nor deep tissues (Fig 2b) in either TBI or craniotomy alone groups. We observed significant increases in hyaluronan in both superficial (Fig 2a) and deep tissue (Fig 2b) ipsilateral to injury one day after TBI. In contrast, there was a decrease in chondroitin sulfate levels in deep tissue one day after TBI (Fig 2b). These offsetting differences contributed to a lack of overall change in total GAG content one day after TBI in either superficial or deep tissue (Fig 2a, b).

Notably, at day 7, we observed increases in all GAG subtypes in superficial ipsilateral tissue after TBI (Fig 2c). There were no significant changes in GAG levels in superficial or deep tissues 7 days after craniotomy (Fig. 2c, d) nor deep tissues 7 days after TBI (Fig. 2d). A summary of significant changes in GAG content after TBI is provided in Table 1. These observations suggest ECM scaffolding modifications at the site of injury occur rapidly after TBI as evidenced by increased hyaluronan in both superficial and deep ipsilateral tissue within 24h. The deep tissue decreases in chondroitin sulfate at 24 h may reflect

acute downregulation of chondroitin sulfate containing proteoglycans [32] and could serve to temper the local inflammatory response. The superficial increases in all GAG subtypes at 7d coincides with timing of glial scar formation expected in this injury model [33].

Traumatic brain injury evokes changes in sulfation of heparan and chondroitin sulfate

It is well established that the precise sulfation sequences of sulfated GAGs play a major role in their biological activity[23, 34–36]. Accordingly, we next assessed changes in constituent disaccharide subtype percentages of heparan and chondroitin sulfate after TBI (Table 2). Specifically, we compared the proportion of disaccharide subtypes of heparan and chondroitin sulfate between ipsilateral and contralateral tissues post-TBI, allowing for paired comparisons within groups. We found a significant decrease of N-sulfated heparan sulfate in ipsilateral tissue at day one, the acute phase of the traumatic injury, with no significant changes at day 7. We also observed in ipsilateral compared to contralateral superficial tissue significant decreases in *4S*, *2S/4S*, and increases in *0S* chondroitin sulfate one day after TBI and decreases in *2S/4S* chondroitin sulfate at day 7 post-TBI. While shifts in chondroitin sulfate sulfation at early time points were generally subtle, we observed a substantial increase in unsulfated chondroitin sulfate within one day of injury that counterbalanced the loss of the sulfated disaccharide subtypes. Collectively, our results suggest two non-mutually exclusive conclusions: [I] rapid *de novo* synthesis of unsulfated chondroitin sulfate may replace degraded *4S* and *2S/4S*-enriched chondroitin sulfate, and/or [II] local upregulation of the chondroitin sulfate-specific sulfatases, arylsulfatase B and iduronate-2-sulfatase[37]. Interestingly, the disaccharide content of both heparan and chondroitin sulfate normalized by day 7, suggesting a homeostatic pressure to reestablish a basal GAG environment after injury.

Circulating GAG levels are not affected by either traumatic brain injury or polytrauma

We previously discovered that systemic endothelial glycocalyx-derived GAGs directly penetrate the brain barrier and impact cognition after recovery from sepsis[7, 8]. Furthermore, there is substantial evidence for significant endothelial injury during TBI with polytrauma [28, 29, 38, 39]. Thus, we next evaluated whether GAG levels increase in the bloodstream in mice after TBI or humans after combined TBI and severe polytrauma. Surprisingly, we did not observe changes in plasma levels of GAGs in our murine model of TBI (Fig. 3a) nor in humans with severe polytrauma and TBI (Fig. 3b) compared to respective controls. These observations suggest that local upregulation of GAG synthesis, rather than direct brain penetration of circulating GAGs, is likely responsible for observed GAG increases in injured tissue after TBI.

Post-traumatic transcriptional changes associated with GAG alterations

To further investigate the mechanisms responsible for increases in GAG content after injury (as summarized in Table 1), we performed bulk transcriptomic analysis on superficial tissue collected 7 days post-TBI. Comparisons were made between ipsilateral (injured) and contralateral (uninjured) tissue. A total of 1657 genes were found to be differentially regulated (Fig. 4; microarray data is available with GEO accession number GSE242025). We performed Gene Set Enrichment Analysis (GSEA) using GSEA software (gsea-msigdb.org/gsea/index.jsp)[40, 41] to identify molecular pathways that were differentially regulated in

ipsilateral compared to contralateral tissue (Table 3). This analysis revealed that of 1039 total gene sets analyzed, 31 were significantly upregulated and 6 downregulated in ipsilateral compared to contralateral tissue based upon a strict Family-Wise Error Rate (FWER) cutoff of 0.05. “Extracellular Matrix Organization” and “Extracellular Matrix Proteoglycans” were two of the most significantly upregulated gene sets (both FWER p-value < 0.001) ranked by Normalized Enrichment Scores (NES). Based upon these GSEA results, we next compared genes associated with GAG biosynthesis (list aggregated from the Kyoto Encyclopedia of Genes and Genomes database entries for biosynthesis and degradation pathways of heparan sulfate, chondroitin sulfate, and hyaluronan; http://www.genome.jp/kegg; Table 4). We found a modest, yet significant upregulation of hyaluronan synthase 2 (Has2) in injured tissue, consistent with increases in hyaluronan content at the site of TBI (Table 4). We also observed a nearly 500% increase in N-deacetylase/N-sulfotransferase 4 (Ndst4), an enzyme known to catalyze N-deacetylation and N-sulfation of intracellular unsulfated heparan sulfate chains[42] (Table 4). There were no other transcriptional changes in biosynthesis or degradation genes that could account for observed increases in heparan sulfate nor chondroitin sulfate 7 days post-TBI. (see Supplementary Table 1 for full list of GAG biosynthesis and degradation enzymes included in our analyses).

As transcriptional changes in neither GAG biosynthesis nor degradation genes could account for the observed elevation in heparan sulfate or chondroitin sulfate, we next evaluated changes in the transcription of proteoglycans[43]. We found significant changes in injured brain tissue in heparan sulfate-containing glypican-3 (231% increase), chondroitin/dermatan sulfate containing decorin (731% increase), and the chondroitin sulfate-containing proteoglycan Plexin domain containing 1 gene (49% decrease; see Table 5).

No other proteoglycans were significantly up- nor downregulated (see Supplementary Table 1 for full proteoglycan gene list). Increases in decorin and glypican-3 transcription at the site of TBI were confirmed via immunofluorescence microscopy 7 days post-TBI. (Fig. 5, representative images; see Supplementary Figs. 1,2 for all images). These results suggest that upregulation of decorin and glypican-3 may be mechanistically responsible for increased GAG content within superficial tissue 7d after TBI.

A genetic background lacking decorin worsens motor deficits after traumatic brain injury

We next sought to determine whether observed proteoglycan changes at the site of injury affect function after TBI. It has previously been reported that decorin upregulation and treatment with recombinant decorin can mitigate scar formation and positively impact functional recovery after TBI[44–46]. To address this possibility, we performed multimodal behavioral assessment in $Dcn^{+/+}$ and $Dcn^{-/-}$ mice 7 days post-TBI or post-craniotomy. In open field testing, there were no changes in total mobility in any group, but following TBI, mice of both genotypes demonstrated a significant increase in anxiety-like behavior (represented by decreased time in the center of the arena); this effect was not modified by genotype (Fig. 6a). In a balance beam task, we found that gross motor coordination was impaired after TBI and was exacerbated in $Dcn^{-/-}$ *mice* (Fig. 6b). In contrast, rotarod testing demonstrated deficits in motor learning after TBI that was consistent in both genotypes (Fig. 6c, see Supplementary Table 2 for complete statistics).

Together these findings suggest that TBI may promote anxiety-like behavior and deficits in both motor learning and fine-motor ability. However, local upregulation of decorin may decrease severity of fine-motor deficits without an impact on anxiety-like behavior nor motor learning.

Discussion

We sought to delineate the complexity and functional impact of brain ECM GAG remodeling after TBI. We observed substantial tissue injury and robust functional deficits in mice after CCI, which is consistent with human studies of severe TBI demonstrating volume reductions in deep brain structures and persistent motor deficits[47–49]. Due to the severity of injury in our murine model, it is important to acknowledge that our results may not be generalizable to mild forms of TBI associated with limited radiographic tissue injury.

While changes in proteoglycans, specific GAG epitopes (measured with chondroitin sulfate-specific antibodies), and GAG sulfation characteristics have been previously studied[14–16, 32], this work is the first to directly quantify GAG content and sulfation patterns via HPLC-MS/MS in injured and uninjured brain tissues after TBI. Our analyses revealed dramatic increases in heparan sulfate, chondroitin sulfate, and hyaluronan in the injured hemisphere (ipsilateral, superficial) when compared to the craniotomy-alone and uninjured hemispheres (contralateral, both TBI and craniotomy-alone) 7d after TBI. Unlike our previous observations in sepsis, endothelial glycocalyx-derived GAG fragments were not found to be released into circulation after TBI in a murine model nor in patients afflicted with combined severe trauma and TBI (those at high risk for GAG release due to endothelial injury and glycocalyx degradation). GSEA of bulk transcriptomic analyses comparing injured (ipsilateral) and uninjured (contralateral) hemispheres in mice after TBI demonstrated that ECM remodeling and proteoglycan pathways were enriched in injured tissue. Subsequent analyses of these transcriptomics data revealed GAG increases at the site of injury are potentially driven by upregulation of GAG biosynthesis machinery (Has2, hyaluronan) and proteoglycans (glypican-3 and decorin).

Our results diverge from prior work in important ways. Contrary to our *a priori* hypothesis, we did not observe an increase in circulating glycosaminoglycans after TBI in mice nor in humans after TBI with severe polytrauma. This is in contrast to a single pre-clinical study reporting an increase in serum syndecan-1 (a major heparan sulfate-containing proteoglycan constituent of the endothelial glycocalyx) after TBI[29]. This prior work utilized a murine model of TBI with significant short-term mortality (nearly 20%) compared to no observed mortality in our study, suggesting that a difference in severity of illness may have driven differential endothelial injury. Despite a less severe injury, we did observe significant increases in all GAGs at the site of TBI after 7 day and relevant functional deficits. Our work is also inconsistent with prior human studies that have reported an increase in plasma syndecan-1[28] and GAGs (measured via ELISA-based assays)[38, 39] early after polytrauma and/or TBI. However, they are consistent with a previous report by our group demonstrating that patients after traumatic injury had significantly lower levels of urinary GAGs than patients with sepsis[25]. Based upon these discordant results, we cannot definitively conclude that circulating GAGs do not contribute to increased brain ECM GAG levels after TBI.

While we can conclude that circulating GAGs are not necessary to increase content at the site of injury, it remains feasible that in a some pre-clinical models and a subset of patients with both severe endothelial injury and TBI, circulating GAGs released from the endothelial glycocalyx may worsen functional outcomes as in sepsis[7, 8].

While our findings do not support a central role for circulating, endothelial-derived GAGs in promoting poor outcomes after TBI, our investigations did reveal putative mechanisms for post-injury GAG changes within the brain that may have functional consequences. We found that upregulation of Has2 may be responsible for increases in hyaluronan after TBI, consistent with prior studies focused on the spatiotemporal dynamics of hyaluronan synthesis during brain injury[18]. While not measured directly in this study, distribution of hyaluronan fragment size is known to be central to its biologic consequences[50]. Furthermore, post-translational regulation of Has2 is critical to its effects on hyaluronan biosynthesis, information that was not captured by our transcriptomics approach[51]. Accordingly, significant future work will be necessary to fully elucidate the dynamic changes and consequences of hyaluronan levels we have observed after TBI. We also observed that transcriptional upregulation of glypican-3 and decorin may be responsible for increases in heparan sulfate and chondroitin sulfate content, respectively, within the brain after TBI. While constitutive *Has2* and *Gpc3* deficiency cause mid-gestational or perinatal death in mice, *Dcn*$^{-/-}$ *mice* do survive to maturity and have been shown to be phenotypically normal aside from skin and tendon fragility[52–54]. Availability of *Dcn*$^{-/-}$ *mice* allowed us to determine the contribution of decorin upregulation to post-TBI functional outcomes. Although they have not yet been developed, conditional *Has2* and *Gpc3* null mice could be generated to specifically test their roles in post-TBI recovery. Additionally, as non-specific hyaluronan synthase inhibitors are available (e.g. 4-methylumbelliferone[55]), the impact of these drugs in pre-clinical models of TBI should be evaluated in future investigations. Notably, this is the first report to identify *Gpc3* upregulation (a proteoglycan that has primarily been studied in the context of cancer and developmental biology[53, 56]) in any form of brain injury.

Decorin has previously been found to reduce scar formation, inflammation, and oxidative stress after TBI [44, 45]. Further, selective conditional knockout of decorin within the amygdala attenuates a post-traumatic stress disorder-like phenotype in mice after TBI [46]. Through our unbiased bulk transcriptomics analysis of the brain after TBI, we similarly identified decorin as a potential a key player in the biologic response to injury. Further, the exacerbation of fine-motor motor deficits we observed in *Dcn*$^{-/-}$ *mice* after TBI is concordant with prior reports suggesting its adaptive benefit and supports an overarching hypothesis that endogenous decorin upregulation attenuates TBI-related injury. As such, additional studies are warranted to further explore decorin as a potential therapeutic for the treatment of this devastating condition.

Conclusions

In summary, we provide novel insight into the spatiotemporal dynamics of GAGs in the brain ECM after TBI and the mechanistic drivers of these changes. Additionally, we

offer evidence of an adaptive role for decorin upregulation at the sites of traumatic injury supporting the potential for decorin as a therapy to improve functional outcomes after TBI.

Experimental Procedures

Animal Experiments

All animal experiments were performed with approval from the institutional animal care and use committee of the University of Colorado Office of Laboratory Animal Resources in accordance with the *Institutional Animal Care and Use Committee Guidebook* published by the NIH Office of Laboratory Animal Welfare and the Animal Research Reporting of In Vivo Experiments (ARRIVE) Guidelines [57]. Male and female 8- to 16-week-old C57BL/6 mice purchased from Charles River Laboratories (Wilmington, MA). We utilized a well characterized *Dcn*$^{-/-}$ mice, which have a mild skin fragility phenotype that allows their utilization in various biological settings[54].

Human Subjects

Plasma samples were collected as part of a prospective database, the Trauma Activation Protocol (TAP). TAP includes all trauma activation patients from 2015 to 2022 at the Ernest E. Moore Shock Trauma Center at Denver Health, an American College of Surgeons verified and Colorado state certified academic Level-1 trauma center. TAP was approved by the Colorado Multiple Institution Review Board (COMIRB# 13–3087 “An Observational Study of the Causative Factors and Molecular Mechanisms of Trauma-induced Coagulopathy”) and performed under waiver of consent. Criteria for inclusion in TAP were adult (≥18 years old) trauma activation patients. The criteria for activation are traumatic injury with any of the following: 1) Glasgow Coma Scale (GCS) < 8 with presumed thoracic, abdominal or pelvic injury, 2) respiratory compromise with presumed thoracic, abdominal, or pelvic injury, 3) blunt trauma with systolic blood pressure (SBP) < 90 mm Hg, 4) mechanically unstable pelvic injury, 5) penetrating injuries to neck and/or torso with SBP < 90 mm Hg or that require endotracheal intubation, or 6) amputation proximal to the ankle or wrist. Exclusion criteria include any patient < 18 years, patients whose initial blood sample is not collected within one hour of injury, infusion of blood products prior to collection of blood samples, documented chronic liver disease (total bilirubin > 2.0 mg/dL or advanced cirrhosis discovered on laparotomy), known inherited defects of coagulation function (e.g., hemophilia or Von Willebrand’s disease), and patients who are pregnant or incarcerated.

Patients categorized as “no TBI with mild trauma” were defined by an injury severity score (ISS) of less than 9 with a GCS score of 15 (completely normal cognition) prior to hospital arrival. Patients categorized as having “TBI and severe trauma” were defined by an ISS greater than or equal to 9 and a GCS of less than or equal to 6 (severe cognitive abnormalities) prior to hospital arrival. The ISS is a standard scale used to assess degree of traumatic injury with mild injury being defined by a score of less than 9 and a maximum severity score of 75[58]. The GCS ranges from 3 to 15 with scores of 3 to 8 suggestive of severe injury and maximum score of 15 being consistent with normal cognition [59].

Murine Controlled Cortical Impact Injury Model

Surgical procedures for the CCI injury model of TBI were completed as previously described[60]. Briefly, mice were anesthetized with inhaled isoflurane while secured in a stereotax for the duration of the procedure. A 4mm craniotomy was performed, which was centered 2mm posterior to the coronal suture and 2.7 mm lateral to the sagittal suture on the right hemisphere. The dura was exposed, and a rapid impact was delivered via the Benchmark Stereotaxic Impactor (MyNeurolab, St. Louis, MO, USA) with parameters that produced an impact depth of 2mm. The craniotomy bone flap was replaced and skin sutured after active swelling subsided. All mice received 1mL saline subcutaneously immediately following wound closure. GAG analyses were performed on brain tissues harvested from mice 1d or 7d after CCI or craniotomy-alone.

For brain tissue harvests, mice were anesthetized with 4% isoflurane. A bilateral thoracotomy was performed, and animals were perfused with saline at a rate of 2.5 mL/min via transcardiac puncture. Animals were subsequently decapitated and superficial and deep tissues were taken from both the surgical site and the contralateral brain. Superficial tissue in the 1) ipsilateral brain of craniotomy animals and 2) contralateral brain of both CCI and craniotomy animals was cortical and deep tissue was hippocampal. For ipsilateral tissue from CCI mice, superficial tissue was taken from the injury site at a depth that corresponded to the cortex and deep tissue was from a location immediately below the harvested superficial tissue, approximating the location of the hippocampus. The degree of destruction after CCI did not allow for precise dissection of cortex and hippocampus ipsilateral to injury.

GAG Analysis

GAG analysis of brain tissue and plasma was performed by HPLC-MS/MS as previously described[8, 9]. These analyses were performed on two distinct brain tissue and plasma batches: one at Rensselaer Polytechnic Institute (RPI) and a second at the University of Colorado Anschutz Medical Campus (UC-AMC) using equivalent methods. In Figure 2, brain tissues analyzed at RPI are indicated in blue and those at UC-AMC are indicated in black. Specific injection sequences for brain and plasma samples are included in Supplementary Tables 3 and 4, respectively. Briefly, we first removed lipid from brain tissues with methanol and dichloromethane. We then digested tissues with actinase E (Kaken Pharmaceutical Co; Tokyo, Japan) in 10mM sodium acetate and 5mM calcium acetate at 55°C until complete tissue digestion was achieved. We removed actinase E and extracted GAGs with ion exchange column (Sartorius Vivapure Q; Göttingen, Germany) in the presence of 8M urea to facilitate dissociation of GAGs from proteins. We desalted samples with a 3kDa molecular weight cut-off column and digested extracted GAGs with heparinase I, II, III and chondroitinase ABC overnight. We collected digested GAGs and derivatized with 2-aminoacridone in DMSO:AcOH = 17:3 (by volume) solution and sodium cyanoborohydride. We cleaned samples with C18 resin and analyzed samples with HPLC-MS/MS. Brain tissue results were normalized to the dry weight of each tissue sample. Plasma samples were processed equivalently without delipidation and tissue digestion steps. Results from our murine model were normalized to contralateral craniotomy as two separate batches of mass spectrometry were performed for these experiments, necessitating

an internal control for each batch. Contralateral-craniotomy tissue (either cortical or hippocampal) was chosen for normalization as it was least likely to be affected by surgical procedures. Concordantly, plasma GAG levels were normalized to day 7 craniotomy-alone plasma levels, the time point and experimental condition at which plasma GAGs are most likely to have fully normalized. Notably, previous work by our group has demonstrated that even in models of severe systemic inflammation, endothelial-derived GAGs only circulate for approximately 24 to 48h after injury[8]. GAG quantification in human plasma samples was performed in a single batch, thus quantitative results are reported.

To mitigate experimental error in our HPLC-MS/MS methods, external standards were injected every 5 to 15 samples to account for ion suppression by biological matrix and instrument drift. Reported values were calculated based on the average of those standards injected immediately before and after the sample block injection. For all analyses at UC-AMC, several additional strategies were utilized to decrease bias and control experimental error. Samples were deidentified and injected in a random order. Furthermore, to evaluate and correct for matrix effect, “tech mix”, a mixed sample collected and mixed from every sample for each sample type (brain or plasma) was included in the injection sequence and injected every 5 to 14 samples. Brain tissue data were then adjusted for signal drift using metabodrift[61].

Whole Transcriptome Analysis

Superficial tissue at the site of injury and cortical tissue contralateral to injury were harvested as for GAG measurements. After isolation, tissues were immediately flash frozen in liquid nitrogen in RNAase-free tubes. RNA extraction was performed using a RNAeasy kit per the manufacturer’s instructions (Qiagen; Hilden, Germany). RNA quality and quantity were assessed in each sample using two methods: 260/280 ratio using a Tecan Infinite 200 Pro plate reader (Männedorf, Switzerland) and RNA electropherography using RNA ScreenTape (Agilent; Santa Clara, CA). All samples submitted had high quality RNA with 260/280 ratios of approximately 2.0 and RINe scores greater than or equal to 8.1. A Clariom™ D mouse assay (Affymetrix Thermo Fisher Scientific; Santa Clara, CA) was performed according to the manufacturer’s instructions by the University of Colorado Anschutz Medical Campus Genomics and Microarray Core facility for whole genome transcriptomics profiling. Briefly, single stranded cDNA was prepared from isolated RNA from each sample. Following fragmentation, 5.5 μg of cDNA from each sample was labeled with biotin then hybridized to the GeneChips array. GeneChips were washed and stained in an Affymetrix Fluidics Station 450 then scanned with an Affymetrix Gene Chip Scanner 3000 7G. CEL files were generated using GeneChip Command Console Software. Data were analyzed utilizing the Transcriptome Analysis Console version 4.0 (Thermo Fisher Scientific; Santa Clara, CA) comparing ipsilateral to contralateral superficial tissue and significant differences were considered those transcripts with FDR p-values < 0.05. Volcano plots were generated using GraphPad Prism (Boston, MA). GSEA was performed using software available through the University of California San Diego and the Broad Institute[40, 41]. The human Reactome gene sets database with a Mouse Clariom D Human Ortholog Chip platform was utilized for these analyses. The top 10 upregulated (of 31) and 6 downregulated gene sets with FWER values of less than 0.05 are included in Table 3.

Immunofluorescence

Following perfusion, whole brains were fixed in 4% paraformaldehyde (PFA) for a minimum of 24h then remained in cryoprotection solution until sectioned into 50μm slices using a microtome (SM2010 R Sliding Microtome, Leica.). Slices received three five-minute PBS washes followed by blocking with 5% donkey antiserum in 0.3% Triton in PBS (PBS-T) for 1h at RT. Next, incubation of primary antibodies (Decorin [LF114], 1:200, Kerafast, Boston, MA; Glypican-3 [9C2], 1:500, Invitrogen, Carslbad, CA) was carried out in PBS-T at 4°C overnight, followed by three five-minute PBS washes. This was followed by AlexaFluor 488-conjugated (1:500, Jackson ImmunoResearch, West Grove, PA) secondary antibody incubation for 45 minutes at RT, followed by three 10-minute PBS washes. Lastly, slices were incubated with Hoescht 33342 (1:10,000 in PBS, Tocris, Minneapolis, MN) for 5min, followed by three five-minute PBS washes. Slices were then mounted with hardset medium (VectorLabs, Burlingame, CA) and visualized using a FLUOVIEW FV1200 confocal laser scanning microscope (Olympus, Tokyo, Japan).

Assessment of Murine Anxiety and Motor Function

All behavioral experiments were performed by a blinded experimenter and analyzed in a blinded fashion. These methods have been previously utilized by our group for studies of anxiety and motor dysfunction after injury[60, 62, 63].

Spontaneous Locomotion and Anxiety-Like Behavior (Open field)

Mice were placed into a 10 × 10 × 10cm enclosure equipped with an overhead camera and their spontaneous behavior was recorded for 10 minutes. Percentage of time spent in the center of the arena was compared to time near walls, which was used to measure anxiety-like behavior. Propensity to spend time near edges served as an indication of higher anxiety. Videos were analyzed in an unbiased fashion using AnyMaze software (Stoelting Company; Wood Dale, IL).

Gross Motor Coordination (Balance Beam)

Testing was carried out as previously described by our group[63]. Briefly, mice were placed on an elevated balance beam that tapered from 1.2cm to 0.5cm at the start and end points, respectively. Animals were initially trained to travel directly to a goal enclosed box located at the tapered end of the beam without consideration of missteps (typically requiring 3–5 trials). Once trained, three trials were performed, and videos were captured from below the beam. Videos were manually scored for missteps onto the support ledge.

Motor Learning (Rotarod)

Animals were placed on a rotating beam and their latency to fall was recorded as the rotational speed steadily increased over the course of a 300 second trial. The test consisted of three trials per day for three consecutive days to assess motor learning. The rotations per minute (rpm) began at 4rpm and reached 30rpm by the end of each trial, increasing at single rpm increments. Latencies to fall were recorded by the Rotarod apparatus (Ugo Basile; Gemonio, Italy) and averaged across the three trials for individual animals on each day of

testing. Longer latencies to fall over time (more time on the rotarod device) and retention in ability between days 8 and 9 represents motor learning[62, 64].

Statistics

One-way ANOVA tests with Tukey correction for multiple comparisons were used to compare GAG levels between groups and hemispheres (Fig. 2). Individual, unadjusted two-tailed t-tests were performed to compare heparan sulfate and chondroitin sulfate sulfation percentages by disaccharide subtype between hemispheres in the TBI groups (Table 1). Two-way ANOVA tests were used to compare mouse plasma GAG levels to evaluate effects of both treatment and time (Fig. 3a) and simple t-tests were used to compare human plasma GAG levels between groups (Fig. 3b). Whole transcriptome analysis comparing ipsilateral and contralateral superficial tissue from mice after TBI was performed using a Clariom D Murine Assay and analyzed using the Affymetrix Transcriptome Analysis Console (Thermo Fisher Scientific; Waltham, MA). False Discovery Rate (FDR) p-values less than or equal to 0.05 were considered significant (Fig. 4, Tables 2 and 3). Full transcriptomics results have been uploaded to the NCBI GEO genomics biorepository and can be accessed with accession number GSE242025. Behavioral outcomes were analyzed using either two-way ANOVA (open field and balance beam) or three-way ANOVA (rotarod) tests (see Supplementary Table 2 for summary statistics). All statistical analyses (except transcriptomics analysis) were performed using Graphpad Prism (Boston, MA).

Supplementary Material

Refer to Web version on PubMed Central for supplementary material.

Acknowledgements

The authors would like to acknowledge the contributions of An Doan, Katrina Diener, and Bifeng Gao of the University of Colorado Cancer Center Genomics Core for their assistance with performance of the Clariom D Transcriptomics Assay. The original work in Dr. Iozzo laboratory was in part supported by National Institutes of Health Grants RO1 CA245311 and RO3 CA270830.

Funding

This work was supported by the American Heart Association Career Development Award 932840 (KO) and the National Institutes of Health (NIH), National Heart, Lung and Blood Institute grant K08HL149353 and National Institute on Aging grant R03AG074056 (both granted to JAH).

Abbreviations.

TBI	Traumatic Brain Injury
ECM	Extracellular Matrix
HPLC-MS/MS	High performance liquid chromatography tandem mass spectrometry
Has2	Hyaluronan Synthase 2

References

1. Nguyen R, Fiest KM, McChesney J, Kwon CS, Jette N, Frolkis AD, Atta C, Mah S, Dhaliwal H, Reid A, Pringsheim T, Dykeman J, Gallagher C. The International Incidence of Traumatic Brain Injury: A Systematic Review and Meta-Analysis. Can J Neurol Sci 2016;43(6):774–85. Epub 2016/09/28. doi: 10.1017/cjn.2016.290. [PubMed: 27670907]
2. Centers for Disease Control and Prevention NCfIPaC. TBI-related Emergency Department Visits, Hospitalizations, and Deaths (EHDSs) 2019 [2/18/2021]. Available from: https://www.cdc.gov/traumaticbraininjury/data/tbi-edhd.html.
3. Poloyac SM, Bertz RJ, McDermott LA, Marathe P. Pharmacological Optimization for Successful Traumatic Brain Injury Drug Development. J Neurotrauma 2020;37(22):2435–44. Epub 2019/03/01. doi: 10.1089/neu.2018.6295. [PubMed: 30816062]
4. George N, Geller HM. Extracellular matrix and traumatic brain injury. J Neurosci Res 2018;96(4):573–88. Epub 2018/01/19. doi: 10.1002/jnr.24151. [PubMed: 29344975]
5. Abdul-Muneer PM, Pfister BJ, Haorah J, Chandra N. Role of Matrix Metalloproteinases in the Pathogenesis of Traumatic Brain Injury. Mol Neurobiol 2016;53(9):6106–23. Epub 2016/11/01. doi: 10.1007/s12035-015-9520-8. [PubMed: 26541883]
6. Iozzo RV, Schaefer L. Proteoglycan form and function: A comprehensive nomenclature of proteoglycans. Matrix Biol 2015;42:11–55. Epub 2015 02 18. doi: 10.1016/j.matbio.2015.02.003. [PubMed: 25701227]
7. Zhang X, Han X, Xia K, Xu Y, Yang Y, Oshima K, Haeger SM, Perez MJ, McMurtry SA, Hippensteel JA. Circulating heparin oligosaccharides rapidly target the hippocampus in sepsis, potentially impacting cognitive functions. Proc Natl Acad Sci USA 2019;116(19):9208–13. [PubMed: 31010931]
8. Hippensteel JA, Anderson BJ, Orfila JE, McMurtry SA, Dietz RM, Su G, Ford JA, Oshima K, Yang Y, Zhang F, Han X, Yu Y, Liu J, Linhardt RJ, Meyer NJ, Herson PS, Schmidt EP. Circulating heparan sulfate fragments mediate septic cognitive dysfunction. J Clin Invest 2019. Epub 2019/02/06. doi: 10.1172/jci124485.
9. Schmidt EP, Li G, Li L, Fu L, Yang Y, Overdier KH, Douglas IS, Linhardt RJ. The circulating glycosaminoglycan signature of respiratory failure in critically ill adults. J Biol Chem 2014;289(12):8194–202. doi: 10.1074/jbc.M113.539452. [PubMed: 24509853]
10. Oshima K, Han X, Ouyang Y, El Masri R, Yang Y, Haeger SM, McMurtry SA, Lane TC, Davizon-Castillo P, Zhang F, Yue X, Vivès RR, Linhardt RJ, Schmidt EP. Loss of endothelial sulfatase-1 after experimental sepsis attenuates subsequent pulmonary inflammatory responses. Am J Physiol Lung Cell Mol Physiol 2019;317(5):L667–l77. Epub 2019/08/29. doi: 10.1152/ajplung.00175.2019. [PubMed: 31461325]
11. Hippensteel JA, Uchimido R, Tyler PD, Burke RC, Han X, Zhang F, McMurtry SA, Colbert JF, Lindsell CJ, Angus DC. Intravenous fluid resuscitation is associated with septic endothelial glycocalyx degradation. Crit Care 2019;23(1):259. [PubMed: 31337421]
12. Properzi F, Carulli D, Asher RA, Muir E, Camargo LM, Van Kuppevelt TH, Ten Dam GB, Furukawa Y, Mikami T, Sugahara K. Chondroitin 6- sulphate synthesis is up- regulated in injured CNS, induced by injury- related cytokines and enhanced in axon- growth inhibitory glia. Eur J Neurosci 2005;21(2):378–90. [PubMed: 15673437]
13. Properzi F, Lin R, Kwok J, Naidu M, van Kuppevelt TH, Ten Dam GB, Camargo LM, Raha-Chowdhury R, Furukawa Y, Mikami T, Sugahara K, Fawcett JW. Heparan sulphate proteoglycans in glia and in the normal and injured CNS: expression of sulphotransferases and changes in sulphation. Eur J Neurosci 2008;27(3):593–604. doi: 10.1111/j.1460-9568.2008.06042.x. [PubMed: 18279312]
14. Bhattacharyya S, Zhang X, Feferman L, Johnson D, Tortella FC, Guizzetti M, Tobacman JK. Decline in arylsulfatase B and Increase in chondroitin 4-sulfotransferase combine to increase chondroitin 4-sulfate in traumatic brain injury. J Neurochem 2015;134(4):728–39. Epub 2015/05/07. doi: 10.1111/jnc.13156. [PubMed: 25943740]
15. Yi JH, Katagiri Y, Susarla B, Figge D, Symes AJ, Geller HM. Alterations in sulfated chondroitin glycosaminoglycans following controlled cortical impact injury in mice. J Comp Neurol 2012;520(15):3295–313. [PubMed: 22628090]

16. Alonge KM, Herbert MJ, Yagi M, Cook DG, Banks WA, Logsdon AF. Changes in Brain Matrix Glycan Sulfation Associate With Reactive Gliosis and Motor Coordination in Mice With Head Trauma. Front Behav Neurosci 2021;15:745288. Epub 2021 10 28. doi: 10.3389/fnbeh.2021.745288. [PubMed: 34776892]

17. Galtrey CM, Fawcett JW. The role of chondroitin sulfate proteoglycans in regeneration and plasticity in the central nervous system. Brain Res Rev 2007;54(1):1–18. Epub 2007 01 11. doi: 10.1016/j.brainresrev.2006.09.006. [PubMed: 17222456]

18. Xing G, Ren M, Verma A. Divergent Temporal Expression of Hyaluronan Metabolizing Enzymes and Receptors with Craniotomy vs. Controlled-Cortical Impact Injury in Rat Brain: A Pilot Study. Front Neurol 2014;5:173. Epub 2014 09 11. doi: 10.3389/fneur.2014.00173. [PubMed: 25309501]

19. Lu J, Goh SJ, Tng PY, Deng YY, Ling EA, Moochhala S. Systemic inflammatory response following acute traumatic brain injury. Front Biosci (Landmark Ed) 2009;14:3795–813. Epub 2009/03/11. doi: 10.2741/3489. [PubMed: 19273311]

20. Vilalta A, Sahuquillo J, Rosell A, Poca MA, Riveiro M, Montaner J. Moderate and severe traumatic brain injury induce early overexpression of systemic and brain gelatinases. Intensive Care Med 2008;34(8):1384–92. Epub 2008/03/20. doi: 10.1007/s00134-008-1056-1. [PubMed: 18350273]

21. McDonald SJ, Sharkey JM, Sun M, Kaukas LM, Shultz SR, Turner RJ, Leonard AV, Brady RD, Corrigan F. Beyond the Brain: Peripheral Interactions after Traumatic Brain Injury. J Neurotrauma 2020;37(5):770–81. Epub 2020/02/12. doi: 10.1089/neu.2019.6885. [PubMed: 32041478]

22. Gaddam SS, Buell T, Robertson CS. Systemic manifestations of traumatic brain injury. Handb Clin Neurol 2015;127:205–18. Epub 2015/02/24. doi: 10.1016/b978-0-444-52892-6.00014-3. [PubMed: 25702219]

23. Siddiqui N, Oshima K, Hippensteel JA. Proteoglycans and glycosaminoglycans in central nervous system injury. Am J Physiol Cell Physiol 2022;323(1):C46–c55. Epub 2022 05 25. doi: 10.1152/ajpcell.00053.2022. [PubMed: 35613357]

24. McDonald SJ, Sun M, Agoston DV, Shultz SR. The effect of concomitant peripheral injury on traumatic brain injury pathobiology and outcome. J Neuroinflammation 2016;13(1):90. Epub 2016 04 26. doi: 10.1186/s12974-016-0555-1. [PubMed: 27117191]

25. Schmidt EP, Overdier KH, Sun X, Lin L, Liu X, Yang Y, Ammons LA, Hiller TD, Suflita MA, Yu Y. Urinary glycosaminoglycans predict outcomes in septic shock and acute respiratory distress syndrome. Am J Respir Crit Care Med 2016;194(4):439–49. [PubMed: 26926297]

26. Schmidt EP, Yang Y, Janssen WJ, Gandjeva A, Perez MJ, Barthel L, Zemans RL, Bowman JC, Koyanagi DE, Yunt ZX, Smith LP, Cheng SS, Overdier KH, Thompson KR, Geraci MW, Douglas IS, Pearse DB, Tuder RM. The pulmonary endothelial glycocalyx regulates neutrophil adhesion and lung injury during experimental sepsis. Nat Med 2012;18(8):1217–23. doi: 10.1038/nm.2843. [PubMed: 22820644]

27. Groswasser Z, Cohen M, Blankstein E. Polytrauma associated with traumatic brain injury: incidence, nature and impact on rehabilitation outcome. Brain Inj 1990;4(2):161–6. doi: 10.3109/02699059009026161. [PubMed: 2331545]

28. Gonzalez Rodriguez E, Cardenas JC, Cox CS, Kitagawa RS, Stensballe J, Holcomb JB, Johansson PI, Wade CE. Traumatic brain injury is associated with increased syndecan-1 shedding in severely injured patients. Scand J Trauma Resusc Emerg Med 2018;26(1):102. Epub 2018 11 21. doi: 10.1186/s13049-018-0565-3. [PubMed: 30463625]

29. Zou Z, Li L, Li Q, Zhao P, Zhang K, Liu C, Cai D, Maegele M, Gu Z, Huang Q. The role of S100B/RAGE-enhanced ADAM17 activation in endothelial glycocalyx shedding after traumatic brain injury. J Neuroinflammation 2022;19(1):46. Epub 2022 02 11. doi: 10.1186/s12974-022-02412-2. [PubMed: 35148784]

30. Shoffstall AJ, Paiz JE, Miller DM, Rial GM, Willis MT, Menendez DM, Hostler SR, Capadona JR. Potential for thermal damage to the blood-brain barrier during craniotomy: implications for intracortical recording microelectrodes. J Neural Eng 2018;15(3):034001. Epub 2017/12/06. doi: 10.1088/1741-2552/aa9f32. [PubMed: 29205169]

31. Cole JT, Yarnell A, Kean WS, Gold E, Lewis B, Ren M, McMullen DC, Jacobowitz DM, Pollard HB, O'Neill JT, Grunberg NE, Dalgard CL, Frank JA, Watson WD. Craniotomy: true sham for

traumatic brain injury, or a sham of a sham? J Neurotrauma 2011;28(3):359–69. Epub 2010/12/31. doi: 10.1089/neu.2010.1427. [PubMed: 21190398]

32. Harris NG, Carmichael ST, Hovda DA, Sutton RL. Traumatic brain injury results in disparate regions of chondroitin sulfate proteoglycan expression that are temporally limited. J Neurosci Res 2009;87(13):2937–50. doi: 10.1002/jnr.22115. [PubMed: 19437549]
33. Chen S, Pickard JD, Harris NG. Time course of cellular pathology after controlled cortical impact injury. Exp Neurol 2003;182(1):87–102. doi: 10.1016/s0014-4886(03)00002-5. [PubMed: 12821379]
34. Afratis N, Gialeli C, Nikitovic D, Tsegenidis T, Karousou E, Theocharis AD, Pavao MS, Tzanakakis GN, Karamanos NK. Glycosaminoglycans: key players in cancer cell biology and treatment. FEBS J 2012;279(7):1177–97. Epub 2012 03 12. doi: 10.1111/j.1742-4658.2012.08529.x. [PubMed: 22333131]
35. Hussein RK, Mencio CP, Katagiri Y, Brake AM, Geller HM. Role of Chondroitin Sulfation Following Spinal Cord Injury. Front Cell Neurosci 2020;14:208. Epub 2020 08 05. doi: 10.3389/fncel.2020.00208. [PubMed: 32848612]
36. Pretorius D, Richter RP, Anand T, Cardenas JC, Richter JR. Alterations in heparan sulfate proteoglycan synthesis and sulfation and the impact on vascular endothelial function. Matrix Biol Plus 2022;16:100121. Epub 2022 09 07. doi: 10.1016/j.mbplus.2022.100121. [PubMed: 36160687]
37. Wang S, Sugahara K, Li F. Chondroitin sulfate/dermatan sulfate sulfatases from mammals and bacteria. Glycoconj J 2016;33(6):841–51. Epub 2016 08 15. doi: 10.1007/s10719-016-9720-0. [PubMed: 27526113]
38. Ostrowski SR, Johansson PI. Endothelial glycocalyx degradation induces endogenous heparinization in patients with severe injury and early traumatic coagulopathy. J Trauma Acute Care Surg 2012;73(1):60–6. doi: 10.1097/TA.0b013e31825b5c10. [PubMed: 22743373]
39. Rahbar E, Cardenas JC, Baimukanova G, Usadi B, Bruhn R, Pati S, Ostrowski SR, Johansson PI, Holcomb JB, Wade CE. Endothelial glycocalyx shedding and vascular permeability in severely injured trauma patients. J Transl Med 2015;13:117. Epub 2015 04 12. doi: 10.1186/s12967-015-0481-5. [PubMed: 25889764]
40. Mootha VK, Lindgren CM, Eriksson KF, Subramanian A, Sihag S, Lehar J, Puigserver P, Carlsson E, Ridderstråle M, Laurila E, Houstis N, Daly MJ, Patterson N, Mesirov JP, Golub TR, Tamayo P, Spiegelman B, Lander ES, Hirschhorn JN, Altshuler D, Groop LC. PGC-1alpha-responsive genes involved in oxidative phosphorylation are coordinately downregulated in human diabetes. Nat Genet 2003;34(3):267–73. doi: 10.1038/ng1180. [PubMed: 12808457]
41. Subramanian A, Tamayo P, Mootha VK, Mukherjee S, Ebert BL, Gillette MA, Paulovich A, Pomeroy SL, Golub TR, Lander ES, Mesirov JP. Gene set enrichment analysis: a knowledge-based approach for interpreting genome-wide expression profiles. Proc Natl Acad Sci U S A 2005;102(43):15545–50. Epub 2005 09 30. doi: 10.1073/pnas.0506580102. [PubMed: 16199517]
42. Aikawa J, Grobe K, Tsujimoto M, Esko JD. Multiple isozymes of heparan sulfate/heparin GlcNAc N-deacetylase/GlcN N-sulfotransferase. Structure and activity of the fourth member, NDST4. J Biol Chem 2001;276(8):5876–82. Epub 2000 11 21. doi: 10.1074/jbc.M009606200. [PubMed: 11087757]
43. Noborn F, Nilsson J, Larson G. Site-specific glycosylation of proteoglycans: A revisited frontier in proteoglycan research. Matrix Biol 2022;111:289–306. Epub 2022 07 15. doi: 10.1016/j.matbio.2022.07.002. [PubMed: 35840015]
44. Logan A, Baird A, Berry M. Decorin attenuates gliotic scar formation in the rat cerebral hemisphere. Exp Neurol 1999;159(2):504–10. doi: 10.1006/exnr.1999.7180. [PubMed: 10506521]
45. Ozay R, Turkoglu E, Gurer B, Dolgun H, Evirgen O, Erguder BI, Hayirli N, Gurses L, Sekerci Z, Yilmaz ER. Does Decorin Protect Neuronal Tissue via Its Antioxidant and Antiinflammatory Activity from Traumatic Brain Injury? An Experimental Study. World Neurosurg 2017;97:407–15. Epub 20161012. doi: 10.1016/j.wneu.2016.09.115. [PubMed: 27744073]
46. Shi Y, Wu X, Zhou J, Cui W, Wang J, Hu Q, Zhang S, Han L, Zhou M, Luo J, Wang Q, Liu H, Feng D, Ge S, Qu Y. Single-Nucleus RNA Sequencing Reveals that Decorin Expression in the Amygdala Regulates Perineuronal Nets Expression and Fear Conditioning Response after

Traumatic Brain Injury. Adv Sci (Weinh) 2022;9(7):e2104112. Epub 2022 01 17. doi: 10.1002/advs.202104112. [PubMed: 35038242]

47. Walker WC, Pickett TC. Motor impairment after severe traumatic brain injury: A longitudinal multicenter study. J Rehabil Res Dev 2007;44(7):975–82. doi: 10.1682/jrrd.2006.12.0158. [PubMed: 18075954]
48. Tomaiuolo F, Carlesimo GA, Di Paola M, Petrides M, Fera F, Bonanni R, Formisano R, Pasqualetti P, Caltagirone C. Gross morphology and morphometric sequelae in the hippocampus, fornix, and corpus callosum of patients with severe non-missile traumatic brain injury without macroscopically detectable lesions: a T1 weighted MRI study. J Neurol Neurosurg Psychiatry 2004;75(9):1314–22. doi: 10.1136/jnnp.2003.017046. [PubMed: 15314123]
49. Serra-Grabulosa JM, Junqué C, Verger K, Salgado-Pineda P, Mañeru C, Mercader JM. Cerebral correlates of declarative memory dysfunctions in early traumatic brain injury. J Neurol Neurosurg Psychiatry 2005;76(1):129–31. doi: 10.1136/jnnp.2004.027631. [PubMed: 15608014]
50. Cyphert JM, Trempus CS, Garantziotis S. Size Matters: Molecular Weight Specificity of Hyaluronan Effects in Cell Biology. Int J Cell Biol 2015;2015:563818. Epub 2015 09 10. doi: 10.1155/2015/563818. [PubMed: 26448754]
51. Parnigoni A, Viola M, Karousou E, Rovera S, Giaroni C, Passi A, Vigetti D. Hyaluronan in pathophysiology of vascular diseases: specific roles in smooth muscle cells, endothelial cells, and macrophages. Am J Physiol Cell Physiol 2022;323(2):C505–c19. Epub 2022 06 27. doi: 10.1152/ajpcell.00061.2022. [PubMed: 35759431]
52. Camenisch TD, Spicer AP, Brehm-Gibson T, Biesterfeldt J, Augustine ML, Calabro A, Jr., Kubalak S, Klewer SE, McDonald JA. Disruption of hyaluronan synthase-2 abrogates normal cardiac morphogenesis and hyaluronan-mediated transformation of epithelium to mesenchyme. J Clin Invest 2000;106(3):349–60. doi: 10.1172/jci10272. [PubMed: 10930438]
53. Cano-Gauci DF, Song HH, Yang H, McKerlie C, Choo B, Shi W, Pullano R, Piscione TD, Grisaru S, Soon S, Sedlackova L, Tanswell AK, Mak TW, Yeger H, Lockwood GA, Rosenblum ND, Filmus J. Glypican-3-deficient mice exhibit developmental overgrowth and some of the abnormalities typical of Simpson-Golabi-Behmel syndrome. J Cell Biol 1999;146(1):255–64. doi: 10.1083/jcb.146.1.255. [PubMed: 10402475]
54. Danielson KG, Baribault H, Holmes DF, Graham H, Kadler KE, Iozzo RV. Targeted disruption of decorin leads to abnormal collagen fibril morphology and skin fragility. J Cell Biol 1997;136(3):729–43. doi: 10.1083/jcb.136.3.729. [PubMed: 9024701]
55. Kakizaki I, Kojima K, Takagaki K, Endo M, Kannagi R, Ito M, Maruo Y, Sato H, Yasuda T, Mita S. A novel mechanism for the inhibition of hyaluronan biosynthesis by 4-methylumbelliferone. Journal of Biological Chemistry 2004;279(32):33281–9. [PubMed: 15190064]
56. Shimizu Y, Suzuki T, Yoshikawa T, Endo I, Nakatsura T. Next-Generation Cancer Immunotherapy Targeting Glypican-3. Front Oncol 2019;9:248. Epub 2019 04 10. doi: 10.3389/fonc.2019.00248. [PubMed: 31024850]
57. Kilkenny C, Browne WJ, Cuthill IC, Emerson M, Altman DG. Improving bioscience research reporting: the ARRIVE guidelines for reporting animal research. PLoS Biol 2010;8(6):e1000412. [PubMed: 20613859]
58. Baker SP, O'Neill B, Haddon W, Jr., Long WB. The injury severity score: a method for describing patients with multiple injuries and evaluating emergency care. J Trauma 1974;14(3):187–96. Epub 1974/03/01. [PubMed: 4814394]
59. Teasdale G, Jennett B. Assessment of coma and impaired consciousness. A practical scale. Lancet 1974;2(7872):81–4. Epub 1974/07/13. doi: 10.1016/s0140-6736(74)91639-0. [PubMed: 4136544]
60. Clevenger AC, Kim H, Salcedo E, Yonchek JC, Rodgers KM, Orfila JE, Dietz RM, Quillinan N, Traystman RJ, Herson PS. Endogenous Sex Steroids Dampen Neuroinflammation and Improve Outcome of Traumatic Brain Injury in Mice. J Mol Neurosci 2018;64(3):410–20. Epub 2018 02 15. doi: 10.1007/s12031-018-1038-x. [PubMed: 29450697]
61. Thonusin C, IglayReger HB, Soni T, Rothberg AE, Burant CF, Evans CR. Evaluation of intensity drift correction strategies using MetaboDrift, a normalization tool for multi-batch metabolomics data. J Chromatogr A 2017;1523:265–74. Epub 2017 09 09. doi: 10.1016/j.chroma.2017.09.023. [PubMed: 28927937]

62. Gould EA, Busquet N, Shepherd D, Dietz RM, Herson PS, de Souza FMS, Li A, George NM, Restrepo D, Macklin WB. Mild myelin disruption elicits early alteration in behavior and proliferation in the subventricular zone. Elife 2018;7:e34783. [PubMed: 29436368]

63. Moreno M, Minjarez C, Vigil J, Orfila JE, Schmidt R, Burch A, Carter DJ, Kubesh M, Yonchek J, Dietz RM, Quillinan N. Differences in hippocampal plasticity and memory outcomes in anterior versus posterior cerebellar stroke. Neurobiol Dis 2022;168:105701. Epub 2022 03 23. doi: 10.1016/j.nbd.2022.105701. [PubMed: 35337949]

64. Shiotsuki H, Yoshimi K, Shimo Y, Funayama M, Takamatsu Y, Ikeda K, Takahashi R, Kitazawa S, Hattori N. A rotarod test for evaluation of motor skill learning. J Neurosci Methods 2010;189(2):180–5. Epub 2010 03 30. doi: 10.1016/j.jneumeth.2010.03.026. [PubMed: 20359499]

Highlight

- Quantification of tissue glycosaminoglycans via mass spectrometry provides unique insight into extracellular matrix remodeling after TBI.
- Decreases in N-sulfated heparan sulfate, 4S and 2S/4S chondroitin sulfate, and increases in 0S chondroitin sulfate were observed 24h after injury, which normalized 7d after injury.
- Increases in total heparan sulfate, chondroitin sulfate, and hyaluronan were observed at the site of injury after 7d.
- Unbiased transcriptomics analyses revealed upregulation of the proteoglycans glypican-3 and decorin, and the biosynthesis enzyme hyaluronan synthase-2 at 7d post-injury. These transcriptional changes may be responsible for observed increases in glycosaminoglycans.
- Behavioral assessment of *Dcn*$^{-/-}$ mice 7d post-injury suggests a protective role for decorin upregulation following TBI.

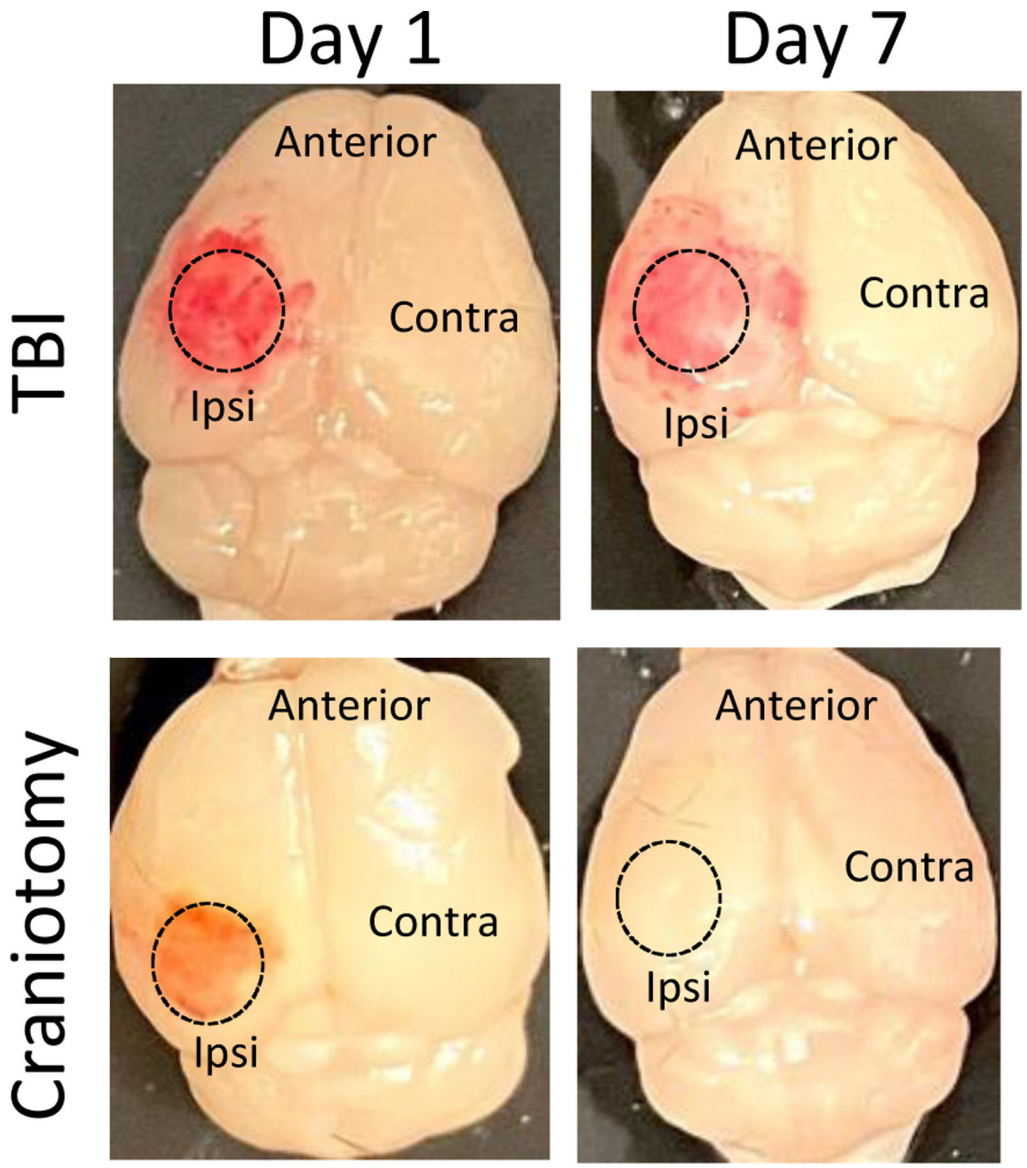

Figure 1. Gross pathologic changes observed with a severe controlled cortical impact model of traumatic brain injury (TBI) compared to craniotomy-alone.

Representative images of brains post-TBI (top) or craniotomy (bottom). Significant hemorrhage and a tissue defect were consistently observed post-TBI at both days 1 and 7. Craniotomy brains were found to have mild erythema at day 1 ipsilateral to surgery, which resolved by day 7. *Ipsi = ipsilateral to surgery; Contra = contralateral to surgery; Dashed circle = site of cortical impact and/or craniotomy.*

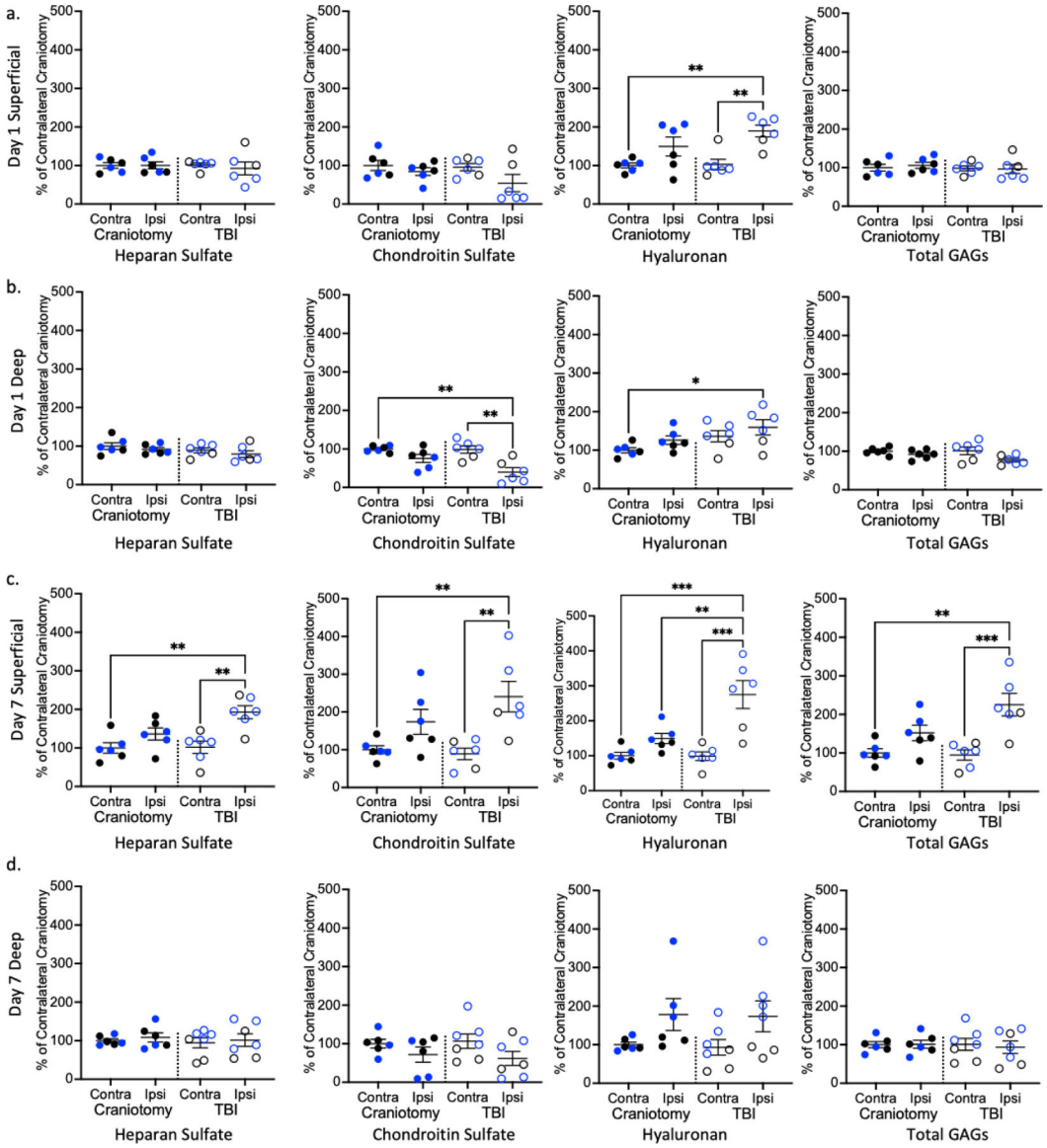

Figure 2. Glycosaminoglycan tissue levels one and seven days after craniotomy or TBI.

High performance liquid chromatography, tandem mass spectrometry was used to measure glycosaminoglycan (GAG) levels (including heparan sulfate, chondroitin sulfate, and hyaluronan) in (a,c) superficial and (b,d) deep tissue harvested 1d and 7d after craniotomy or TBI. Tissue GAG levels were measured both ipsilateral and contralateral to craniotomy or TBI. Each data point represents an experimental animal. *Blue and black symbols indicate different experimental batches performed at different sites. n=6–7 per group.* * $p < 0.05$, ** $p < 0.01$, *** $p < 0.001$ *based upon one-way ANOVA with Tukey correction for multiple comparisons.*

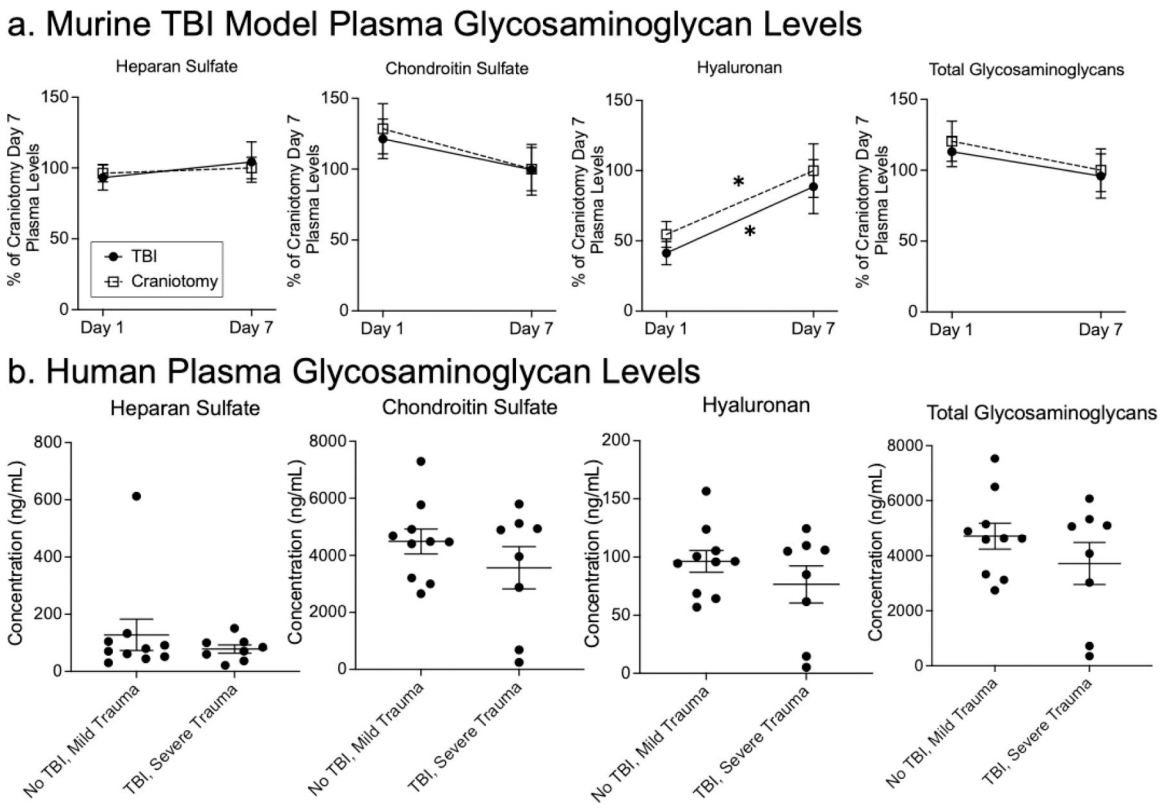

Fig. 3. Plasma glycosaminoglycan levels after TBI in a murine model and humans.

a. Circulating glycosaminoglycans were measured in plasma 1d and 7d after TBI (filled box, solid line) or craniotomy (open box, dashed line). Values are normalized to day 7 craniotomy plasma as levels were measured in different mass spectrometry batches. ** $p < 0.05$ based upon two-way ANOVA with multiple comparisons with Tukey correction, n = 6–7 per group.* b. Circulating glycosaminoglycans were measured in plasma collected in the emergency department from patients with TBI and severe polytrauma [defined by a field Glascow Coma Scale (GCS) score <= 6 and traumatic injury (Injury Severity Score (ISS) > 9)] and from patients with mild traumatic injury without TBI (GCS = 15, ISS <= 9). *Comparisons were made using unpaired t-tests, n = 8–10 per group. In both panels error bars represent mean +/− SEM.*

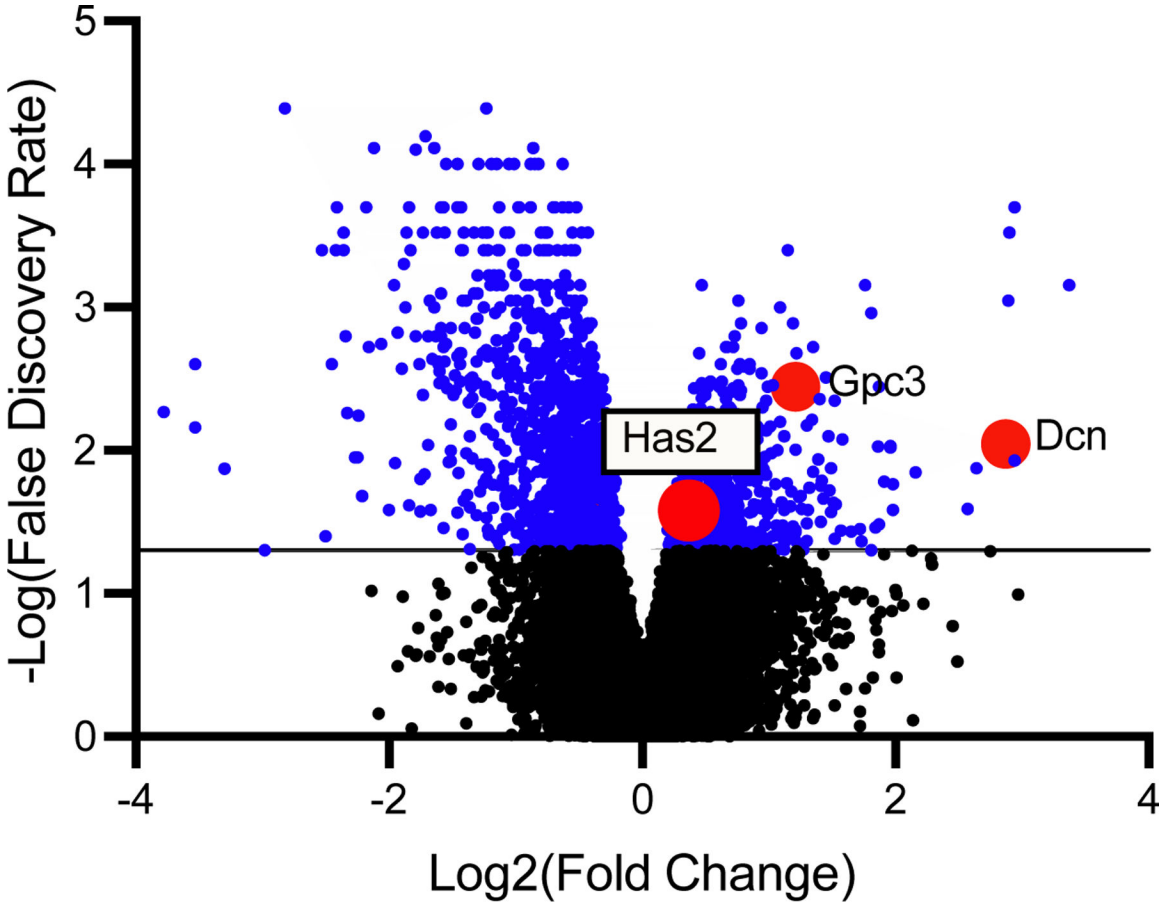

Fig. 4. Volcano plot of bulk transcriptomics analysis of ipsilateral compared to contralateral tissue 7d after TBI.

Decorin *(Dcn),* Glypican-3*(Gpc3)* and Hyaluronan Synthase 2*(Has2)* are highlighted with large red circles. *Solid horizontal line delineates FDR values < 0.05 and all genes highlighted in blue are significantly different when comparing ipsilateral to contralateral tissue.*

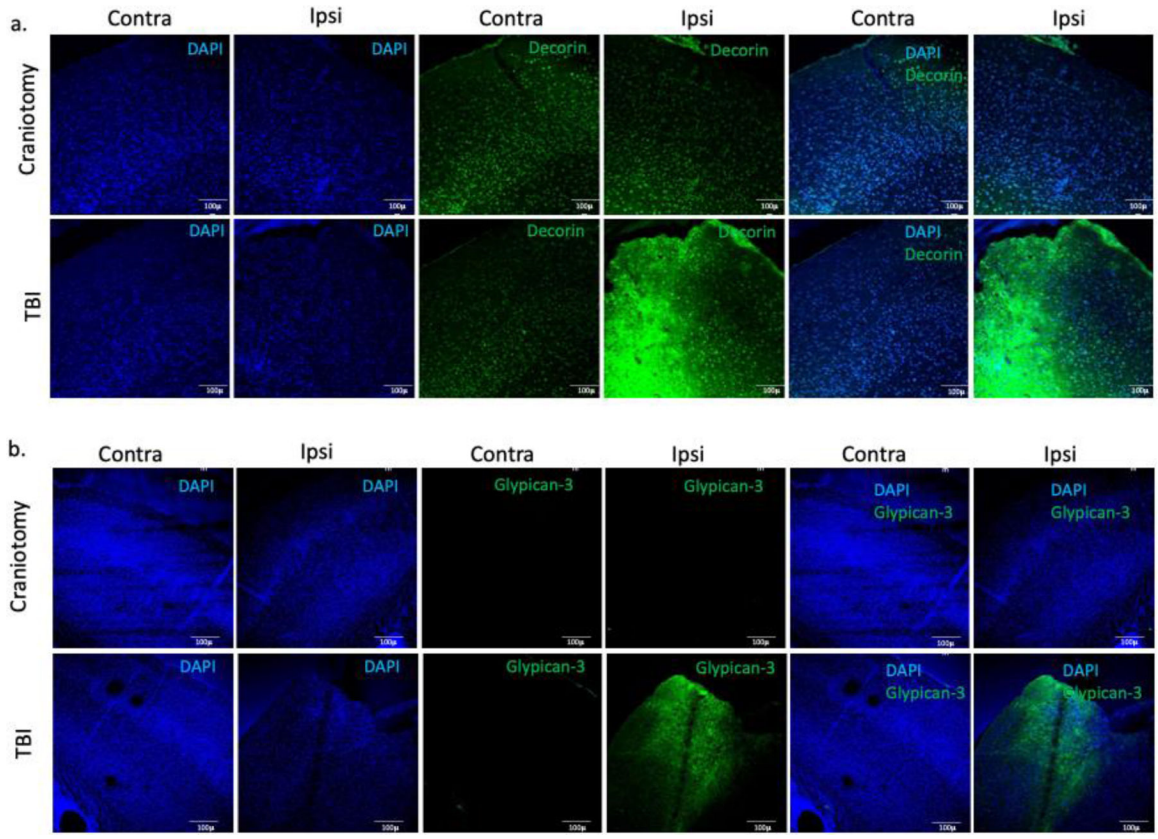

Fig. 5. Verification of proteoglycan changes 7d after TBI by immunofluorescence.

a. Decorin (green) and b. glypican-3 (green) levels are both significantly elevated at the site of injury 7d after TBI. DAPI is included in blue. *Representative images. Scale bars 100 μm.*

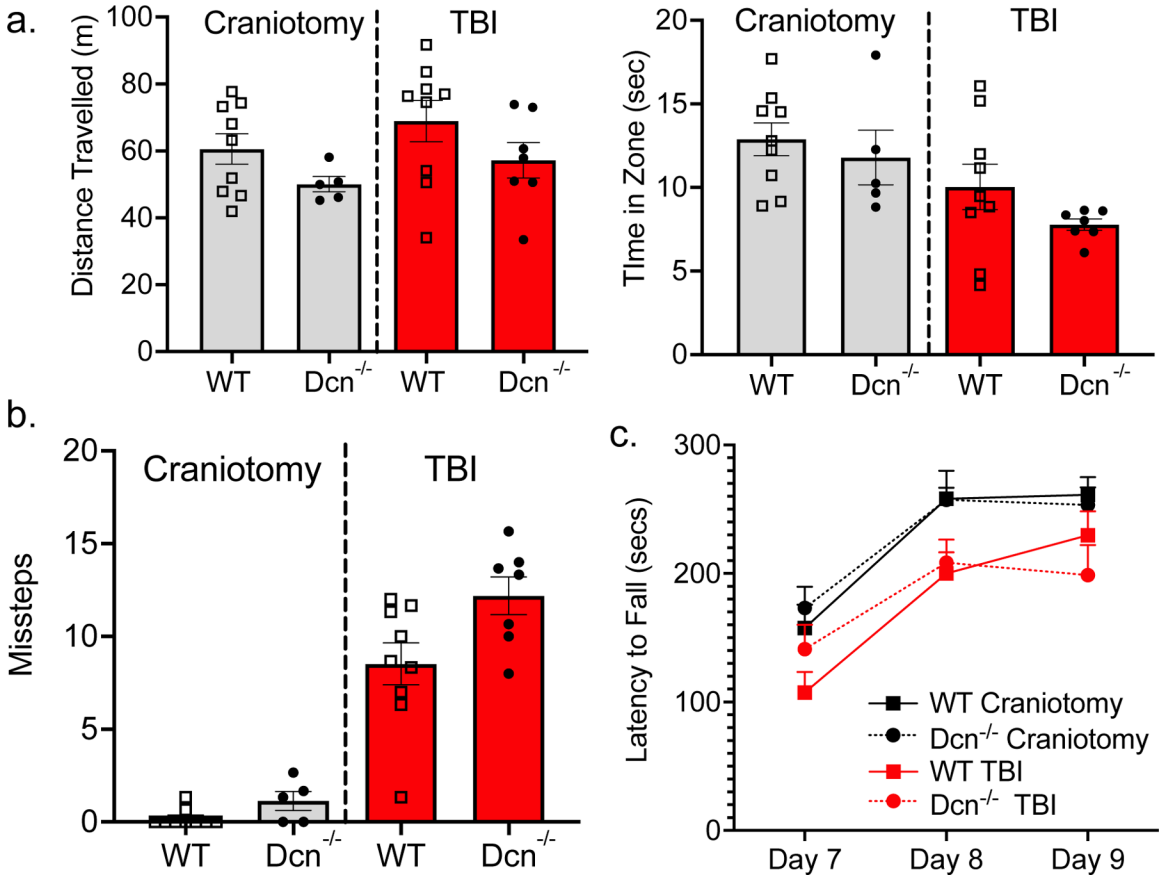

Fig. 6. The effect of global decorin deficiency on general mobility, anxiety-like behavior, gross motor control, and motor learning 7d after TBI.

A behavioral battery consisting of open field mobility (a), balance beam (b), and a serial rotarod task was performed in wild-type and *Dcn*$^{-/-}$ mice beginning 7 days post-TBI. Two- (a,b) or three-way (c) ANOVA tests revealed significant effects of TBI on "Time in Zone" (anxiety-like behavior), balance beam missteps (gross motor coordination), and rotarod testing (motor learning) with no difference in general mobility (distance travelled). Balance beam performance (gross motor coordination) was worsened by decorin knockout genotype after TBI. *n = 5–9 per group.*

Table 1.

Summary of glycosaminoglycan changes after TBI or craniotomy ipsilateral to the surgical procedure.

Day 1		**TBI**	**Craniotomy**
Superficial	Total	-	-
	Heparan Sulfate	-	-
	Chondroitin Sulfate	-	-
	Hyaluronan	↑	-
Deep	Total	-	-
	Heparan Sulfate	-	-
	Chondroitin Sulfate	↓	-
	Hyaluronan	↑	-
Day 7		**TBI**	**Craniotomy**
Superficial	Total	↑	-
	Heparan Sulfate	↑	-
	Chondroitin Sulfate	↑	-
	Hyaluronan	↑	-
Deep	Total	-	-
	Heparan Sulfate	-	-
	Chondroitin Sulfate	-	-
	Hyaluronan	-	-

Table 2.

Effects of TBI on heparan sulfate and chondroitin sulfate disaccharide sulfation percentages.

Comparisons were made between sulfation percentages of ipsilateral and contralateral tissue post-TBI. *Bold font denotes $p < 0.05$ via unadjusted two-tailed t-tests. $n = 6–7$ animals per group.*

			Heparan Sulfate Subtype Mean % (SEM)							
			TriS	**NS6S**	**NS2S**	**NS**	**2S6S**	**6S**	**2S**	**0S**
Day 1	Superficial	Ipsilateral	2.74 (2.50)	2.71 (1.76)	2.79 (1.44)	***4.35 (0.90)***	0.00 (0.00)	3.47 (1.64)	0.43 (0.41)	83.41 (7.06)
		Contralateral	0.76 (0.54)	4.05 (2.20)	4.03 (1.26)	***7.86 (0.75)***	0.00 (0.00)	5.29 (1.54)	0.06 (0.03)	77.81 (4.92)
	Deep	Ipsilateral	8.66 (5.49)	2.65 (1.54)	3.53 (1.61)	***5.62 (0.97)***	0.00 (0.00)	3.29 (1.24)	0.23 (0.18)	75.83 (9.56)
		Contralateral	0.70 (0.42)	4.02 (2.04)	4.27 (0.95)	***9.98 (1.23)***	0.01 (0.00)	5.41 (1.11)	0.52 (0.36)	74.98 (3.57)
Day 7	Superficial	Ipsilateral	7.55 (7.21)	3.78 (1.87)	4.88 (0.82)	7.48 (1.15)	0.03 (0.01)	5.99 (0.92)	0.28 (0.09)	69.86 (8.23)
		Contralateral	14.76 (5.45)	4.21 (1.66)	4.75 (1.18)	5.83 (0.77)	0.02 (0.01)	5.29 (0.76)	0.12 (0.05)	67.18 (8.67)
	Deep	Ipsilateral	4.15 (3.73)	3.31 (1.48)	3.27 (1.20)	4.96 (1.00)	0.01 (0.00)	4.25 (1.55)	0.57 (0.32)	79.35 (7.48)
		Contralateral	5.22 (3.84)	5.10 (2.08)	5.31 (1.14)	7.68 (0.92)	0.02 (0.00)	6.43 (1.01)	0.18 (0.09)	69.85 (5.97)

			Chondroitin Sulfate Subtype Mean % (SEM)							
			TriS	**2S4S**	**2S6S**	**4S6S**	**4S**	**6S**	**2S**	**0S**
Day 1	Superficial	Ipsilateral	0.02 (0.01)	***0.08 (0.03)***	0.21 (0.06)	0.68 (0.20)	***68.83 (9.04)***	1.47 (0.29)	0.05 (0.03)	***28.29 (9.51)***
		Contralateral	0.02 (0.01)	***0.30 (0.06)***	0.21 (0.04)	0.51 (0.11)	***95.60 (0.40)***	1.10 (0.29)	0.06 (0.02)	***1.98 (0.34)***
	Deep	Ipsilateral	0.04 (0.02)	0.30 (0.06)	0.45 (0.1)	0.72 (0.14)	81.19 (5.44)	3.12 (0.60)	0.13 (0.05)	14.31 (5.73)
		Contralateral	0.03 (0.01)	0.28 (0.05)	0.50 (0.12)	0.64 (0.16)	93.12 (0.84)	2.67 (0.14)	0.10 (0.04)	2.97 (0.19)
Day 7	Superficial	Ipsilateral	0.03 (0.01)	***0.14 (0.05)***	0.23 (0.08)	0.39 (0.08)	96.62 (0.64)	1.15 (0.39)	0.16 (0.05)	1.44 (0.30)
		Contralateral	0.06 (0.01)	***0.33 (0.08)***	0.31 (0.08)	0.53 (0.02)	96.07 (0.34)	1.34 (0.33)	0.12 (0.05)	1.79 (0.30)
	Deep	Ipsilateral	0.02 (0.01)	***0.09 (0.03)***	0.18 (0.06)	0.18 (0.07)	95.54 (0.86)	1.05 (0.42)	0.09 (0.04)	3.01 (1.05)
		Contralateral	0.03 (0.01)	***0.29 (0.06)***	0.31 (0.06)	0.40 (0.07)	95.99 (0.48)	1.77 (0.26)	0.12 (0.05)	1.43 (0.28)

Table 3.

Gene set enrichment analysis utilizing Reactome Gene Set Database reveals upregulation of “Extracellular Matrix Organization” and “Extracellular Matrix Proteoglycans” in superficial injured compared to contralateral cortical tissue 7 days post-TBI. *Red indicates upregulated gene sets and blue indicates downregulated gene sets. ES = Enrichment Score, NES = Normalized Enrichment Score, NOM = nominal, FDR = False Discovery Rate, FWER = Family-Wise Error Rate*

Gene Set Name	Gene Set Size	ES	NES	NOM p-val	FDR q-val	FWER p-val
EXTRACELLULAR MATRIX ORGANIZATION	283	0.51	2.35	<0.001	<0.001	<0.001
COMPLEMENT CASCADE	45	0.67	2.34	<0.001	<0.001	<0.001
ELASTIC FIBRE FORMATION	43	0.68	2.34	<0.001	<0.001	<0.001
INTEGRIN CELL SURFACE INTERACTIONS	83	0.60	2.33	<0.001	<0.001	<0.001
DISEASES OF IMMUNE SYSTEM	30	0.73	2.30	<0.001	<0.001	<0.001
EXTRACELLULAR MATRIX PROTEOGLYCANS	76	0.60	2.29	<0.001	<0.001	<0.001
NEUTROPHIL DEGRANULATION	432	0.48	2.28	<0.001	<0.001	<0.001
IMMUNOREGULATORY INTERACTIONS BETWEEN A LYMPHOID AND A NON LYMPHOID CELL	81	0.57	2.26	<0.001	<0.001	<0.001
SYNDECAN INTERACTIONS	27	0.71	2.26	<0.001	<0.001	<0.001
INTERLEUKIN 10 SIGNALING	41	0.65	2.23	<0.001	0.002	0.002
POTASSIUM CHANNELS	102	−0.60	−2.16	<0.001	<0.001	<0.001
VOLTAGE GATED POTASSIUM CHANNELS	43	−0.69	−2.16	<0.001	<0.001	0.001
DAG AND IP3 SIGNALING	40	−0.65	−2.00	<0.001	0.0072	0.022
NUCLEAR EVENTS KINASE AND TRANSCRIPTION FACTOR ACTIVATION	61	−0.61	−2.00	<0.001	0.0061	0.025
NEURONAL SYSTEM	394	−0.48	−1.99	<0.001	0.0057	0.03
NEUREXINS AND NEUROLIGINS	54	−0.61	−1.97	<0.001	0.0069	0.044

Table 4.

Significantly altered glycosaminoglycan biosynthesis enzymes in superficial injured compared to contralateral cortical tissue 7 days post-TBI. *** FDR p value < 0.01*.

Glycosaminoglycan Pathway	Gene Name	Gene Symbol	Function	Fold Change	FDR p-value
HS Biosynthesis	exostoses (multiple)-like 3	Extl3	Backbone elongation	−33%	0.0037
	heparan sulfate 2-O-sulfotransferase 1	Hs2st1	2-Sulfation	−29%	0.0104
	exostoses (multiple)-like 1	Extl1	Backbone elongation	−28%	0.0208
	exostoses (multiple)-like 2	Extl2	Backbone elongation	−25%	0.0223
	N-deacetylase/N-sulfotransferase (heparin glucosaminyl) 4	Ndst4	N-sulfation	490%	0.0257
	exostoses (multiple) 1	Ext1	Backbone elongation	−43%	0.0262
CS + HS Biosynthesis	beta-1,3-glucuronyltransferase 3 (glucuronosyltransferase I)	B3gat3	Backbone elongation	−26%	0.0241
HA Biosynthesis	hyaluronan synthase 2	Has2	Elongation	29%	0.0264

Table 5.

Proteoglycans significantly altered in superficial injured tissue 7d after TBI. *HS = Heparan Sulfate, CS = Chondroitin Sulfate, HA = Hyaluronan.*

Proteoglycan	Gene Symbol	GAG Type(s)	% Change	FDR p-value
glypican 3	Gpc3	HS, CS	231.3%	0.004
decorin	Dcn	CS	731.1%	0.009
Plexin domain containing 1	Plxdc1	CS	−48.6%	0.029